International Journal of Fracture 27 (1985) 187–201.

Mechanics of crack curving and branching – a dynamic fracture analysis

M. RAMULU and A.S. KOBAYASHI

Department of Mechanical Engineering, University of Washington, Seattle, WA 98195, USA

(Received September 1, 1984; in revised form November 8, 1984)

Abstract

A comparative study on crack curving and branching criteria in dynamic fracture mechanics shows that the criteria based on "advanced cracking" concept correlated best with available experimental data. The crack branching criterion requires as a necessary condition, a critical dynamic stress intensity factor, K_{Ib}, and a sufficient condition involving the crack curving criterion. The criteria are used to predict crack curving and crack branching in dynamic photoelastic experiments involving Homalite-100 and polycarbonate fracture specimens, as well as bursting steel and aluminum pipes.

1. Introduction

In a brittle material, a propagating crack will often depart from its original straight trajectory and curve or split into two or more branches or under high state of stress, divide into a river delta crack pattern. This fragmentation of highly loaded, brittle materials is often a succession of multiple branchings of what was initially a single crack. Typical crack curving and crack branching in a glassy polymer, Homalite-100, are shown in Fig. 1.

Despite the number of comprehensive review articles in the general area of dynamic fracture [1–8], elastodynamic analyses of crack curving and branching are few. An approximate analytical solution for a static curved crack with nonvanishing mode II stress intensity factors [9,10], however, is available. Also, dynamic crack branching has been modeled by an elastostatic solution which was used to predict the crack branching angle. An excellent review of static crack branching, and the inaccuracies and inconsistencies involved in such analyses has been provided by Lo [11]. Pärletun [12] and Kalthoff [13] solved numerically, static crack branching problems with a vanishing mode II stress intensity factor.

2. Dynamic crack curving and crack branching

2.1. Crack curving

Experimental observations of crack curving in brittle materials [14–20] show that the curved crack path differs with specimens and loading conditions. For example, the crack path in a bend specimen under impact loading may have a characteristic *S*-shape as the crack approaches the compression side of the specimen [14,15] and a double cantilever beam specimen under wedge loading often yields a gradual curving crack path after fracture initiation [16–19]. Slightly deflected crack paths in single edge notch specimens under uniaxial loading have also been reported in [20].

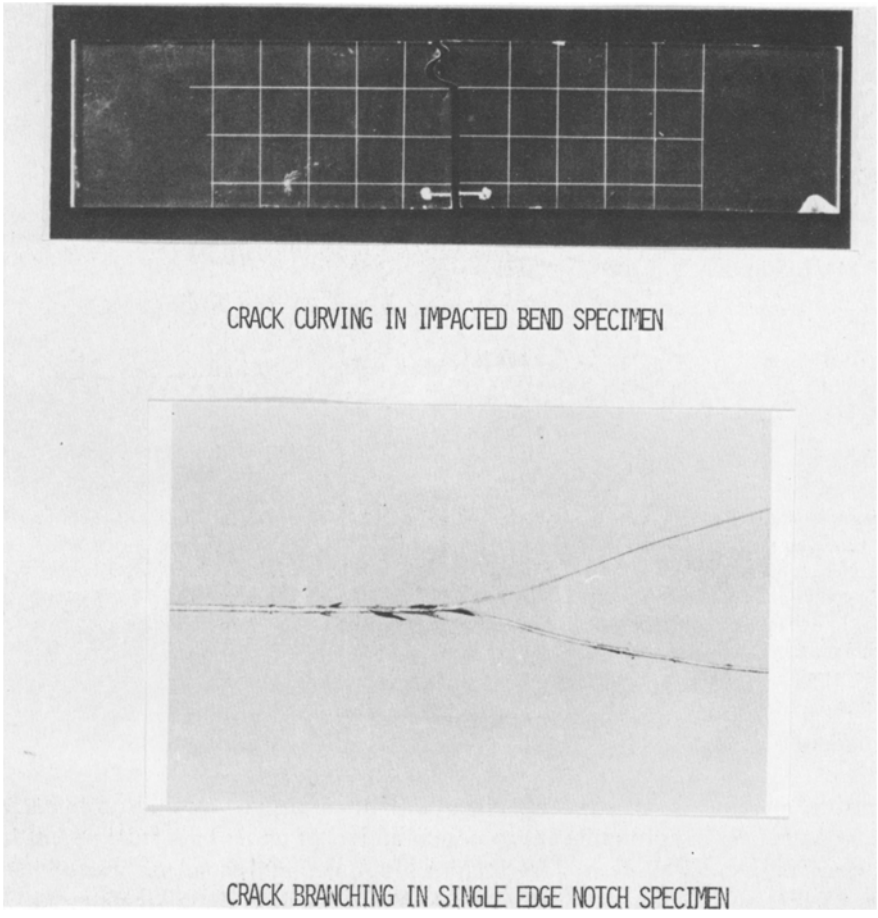

Figure 1. Crack curving and branching.

Directional stability of a straight crack can be enforced either by side grooving or by applying lengthwise compression [17]. Kibler and Roberts [21] showed experimentally, that an increase in the biaxial load increased the apparent fracture toughness and thereby decreased the directional control. Cotterell [18] and A.S. Kobayashi et al. [16] studied the biaxial stress ratio, σ_{xx}/σ_{yy}, at the crack tip and concluded that for straight crack growth, this biaxial stress ratio should be less than unity. Using the same approach, Radon et al. [22] modeled an S-shaped crack as two equivalent-angled cracks or two opposing circular-arc cracks with known modes I and II stress intensity factors, K_{I} and K_{II}, and predicted the curving angles when $K_{\mathrm{II}} = 0$ for varying biaxial stress ratios. In the early work of Benbow and Roesler [17] in 1957, directional stability in square plates was achieved by restricting the movement of the crack faces to parallel outward motion. In DCB specimens, A.S. Kobayashi et al. [16], and Finnie and Saith [23] demonstrated the utility of the lengthwise compression, which is applied parallel to the crack, for crack path stability. More recently, Streit and Finnie [19] developed a directional stability criterion by incorporating the non-singular stress term, σ_{Ox}, which is often referred to as the remote stress component. Directional stability of an extending crack was achieved when a geometrical radius r_0 exceeded or equalled a critical material property r_c. In a series of papers Cotterell [18,24,25], used the crack tip field equations of Williams [26], to show the influence of the nonsingular stress, σ_{0x}, on the directional stability of a propagating crack.

Cotterell concluded that in the absence of K_{II}, the fracture path is stable when $\sigma_{0x} < 0$ and unstable when $\sigma_{0x} > 0$. These conditions, however, were violated in some experiments [20,27,28]. Cotterell and Rice [10] also derived analytically a first order approximation of the necessary conditions for crack curving where the stability of the crack path is governed by the sign of σ_{0x} when $K_{II} = 0$. More recently, Karihaloo et al. [29] derived a curving criterion with non-vanishing dK_{II}/da, when σ_{0x} is zero.

In a recent experimental investigation, Ravi-Chandar and Knauss showed [27,28] that the running crack will have an oscillatory crack path of continuous crack curvings due to the interactions of low amplitude stress waves. In their test specimens, the reflected stress waves from the bottom and top boundaries of the cracked plate impacted the propagating crack tip at different times, changed the crack tip stress field, and induced a change in the crack direction. This experimental evidence suggested that crack curving depends strongly on the specimen geometry and on the loading conditions. Recently, Ramulu and Kobayashi [30] analyzed a series of photoelastic experiments and concluded that crack curving is associated with the stress field acting parallel to the crack tip. This parallel stress appeared to contribute to the crack curving observed by Cotterell [24] and Finnie et al. [19,23]. The latter analyses were elastostatic in nature and no theoretical analyses of dynamic crack curving is available to date. Ravi-Chandar and Knauss [27,28], and Ramulu and A.S. Kobayashi [30], however, characterized dynamic crack curving experimentally, as will be discussed later in this paper.

2.2. *Crack branching*

Crack branching has been frequently observed during the past 18 years of dynamic fracture research at the University of Washington [31], the University of Maryland [32], California Institute of Technology [27], in Europe [13,33–37], and most recently at the University of Rhode Island [38]. Research on crack branching seeks the criterion which controls the onset of bifurcation or crack branching. Among the possibilities considered were the distortion of the crack tip stress field at a critical velocity and the critical stress intensity factor and strain energy release rate at the onset of branching. The size of the fracture mirror zone and the branching event have been correlated and the fracture surface topography and surface roughness have been studied [27,28,31,39]. An increase in the fracture surface roughness prior to branching was observed consistently in all reported investigations.

2.2.1. *Critical velocity criterion*

Long before solutions to elastodynamic crack problems were available, Yoffe [40] presented the steady-state solution for a crack of constant length, moving along a straight line in an infinite two-dimensional medium under remote tractions. Yoffe's pre-branching analysis showed that the maximum circumferential stress, $\sigma_{\theta\theta}$, exhibits two symmetrical maxima along the crack axis at a crack velocity of about $C/C_1 = 0.33$, where C and C_1 are the crack and dilatational wave velocities, respectively. This critical velocity, which shifted the maximum $\sigma_{\theta\theta}$ orientation away from $\theta = 0$, was suggested as promoting crack branching. Later, Craggs [41] showed through the solution of a semi-infinite crack propagating at a constant velocity, that the critical velocity for crack branching should be about $C/C_1 = 0.40$, and reaffirmed Yoffe's criterion on a critical crack velocity. The solution presented by Baker [42] for a propagating crack, which suddenly appears in an infinite plate, showed that $\sigma_{\theta\theta}$ stress is not a principal stress; Baker suggested that the crack should propagate perpendicular to the direction of the maximum principal stress. The physical implications of this maximum principal stress criterion will be discussed later. Validation of the above theoretical solutions, however, was stymied by the lack of

detailed experimental data on the dynamic state of stress in the vicinity of a moving crack tip.

Experimentally observed crack velocities at crack branching are much smaller than the theoretically predicted critical crack velocities for branching. Bowden et al. [43] showed experimentally, that a crack need not propagate at a constant terminal speed before branching occurs, but may accelerate up to the instant of branching, which is then accompanied by a drop of 5 to 10 percent in the crack speed after branching. Döll's [44] experimental observations on plate glass and FK-52 glass indicated that the constant branching velocity of $C/C_1 = 0.28$ and 0.3 was lower than the theoretical value of $C/C_1 = 0.40$. The precise ultrasonic ripple marking technique used by Kerkhoff [36] also showed that the crack velocity decreased about 10 percent in glass immediately after branching, whereas Schardin [45] and Acloque [46] observed no change in crack velocities during branching in plate glass and a 6 percent change in pre-stressed glass, respectively. Crack branching velocities in various steels reported by Carlsson [47–49], Irwin [50], Hahn et al. [51], Congelton et al. [33–35], and Weimer and Rogers [52,53] were less than $C/C_1 = 0.25$. A.S. Kobayashi et al. [31,54,55], and Dally et al. [8,32,56] studied crack branching using dynamic photoelasticity. Ravi-Chandar and Knauss [27,57] used the method of caustics in a glassy polymer, Homalite-100 specimens and observed that crack branching occurred consistently at velocities well below the crack velocity ratio of $C/C_1 = 0.25$. Similar observations were made by Paxson [58] and Doyle [59]. The observed low crack branching velocities, which hardly decreased after branching, showed that a postulated critical crack velocity could not be a prerequisite to crack branching in these materials.

2.2.2. Critical stress intensity criterion

To date, published attempts for analyzing crack branching sought the necessary condition for branching by comparing the stress states prior to and after branching [60,61]. Since crack branching was observed at lower velocities, criticality of other fracture parameters at subcritical lack velocities must be considered [62]. Such parameters could be a critical stress intensity factor or a critical stress in a region ahead of the crack tip. The latter would facilitate development of secondary cracks at an inclination to the propagation direction of the primary crack.

Clark and Irwin [62] concluded that crack branching occurs by advanced cracking, which requires a critical branching stress intensity factor, K_{Ib}. They also stated that the crack velocity approached a limiting velocity before branching. Independently, Congleton et al. [33–35,63] proposed a critical stress intensity factor criterion for crack branching based on advanced cracking. A model of crack branching, which is based on advanced cracking of a Griffith crack, of length 2a, located at a distance, r_c, ahead of the propagating crack formed the micro-mechanic basis of their criterion. Further improvement of this crack branching model was made by Congleton [63], who postulated an advance crack of a penny shape [64]. He then derived a relation between the branching stress intensity factor, K_{Ib}, and the fracture toughness, K_{Ic}. Based on velocity arguments, Congleton suggested that when $n \geqslant 2$, unloading of the main crack is prevented, where n is a constant involved in the assumed relation, $r_c = na$. The critical distance, r_c, could not be determined and thus, $r_c \geqslant 2a$ was assumed. The final linking of the off-axis micro-cracks with the primary crack in the Congleton model resulted in crack branching, and is similar to that assumed by Carlsson [48]. Dally [8], restating the Congleton model, argued that $n = 2$ is somewhat arbitrary and suggested that the "n" be an open parameter which characterizes the size of the fracture process zone at the instant of branching.

The fracture surface topography of mirror, mist, and hackle zone, is clearly visible in ceramics, brittle polymers, and on a larger scale, in rocks. Hence, the fracture mirror zones

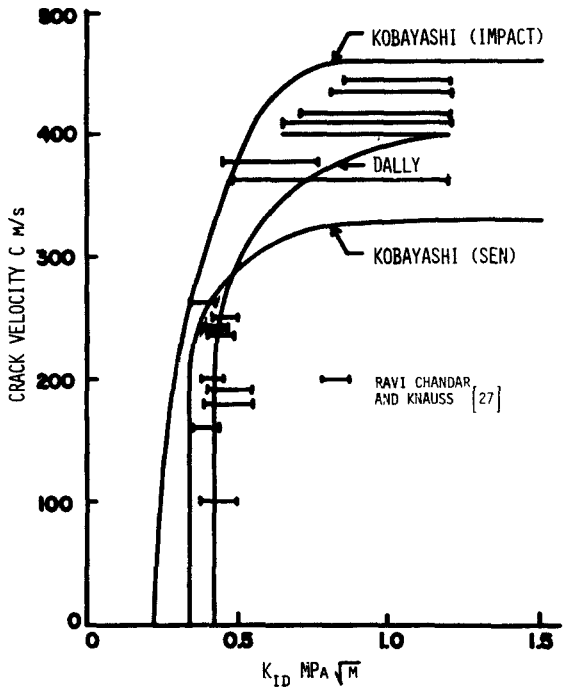

Figure 2. K_{ID} vs. C relations, Homalite-100.

have been utilized to study the strength of ceramics by correlating the algebraic product, A, formed with the mirror radius, $\sqrt{r_m}$, and the fracture stress, σ_f, where A is commonly referred to as the mirror constant and frequently treated as a material constant [65]. The dimensions of the constant are similar to the fracture toughness and thus attempts were made to relate it to the crack branching stress intensity factor, K_{Ib}. The mirror constant, A, has been used in several practical applications, such as to estimate the fracture surface energy [65–67], to determine the magnitudes of the residual stress [67–68], and to predict the flaw size [69–71] in ceramics. However, experimental results obtained by Abdel-Latif et al. [72] and Kishimoto et al. [73] showed that A or K_{Ib} is not a constant but depends on loading conditions. The use of a mirror constant, A, as a branching criterion has two drawbacks: (1) the specimen size does not enter into the calculation of A; and (2) a two-dimensional flaw-shape correction was used. The shape of the mirror, which is a surface flaw, is hard to evaluate because of its three-dimensional shape [73]. The mechanisms of mist, hackle, and crack branching in ceramics have been reviewed extensively by Rice [74].

Available experimental data on crack branching varied from material to material and also appeared to be a function of the test method. Experimental evidence by A.S. Kobayashi et al. [31,75] showed that crack branching consistently occurred in Homalite-100, singled edge notch (SEN) specimens only when K_I reached its maximum value with a negligible K_{II}. This study also showed that the branching stress intensity factor is not a unique material property in agreement with Kishimito et al. [73] but contradicts the results of Congleton [63] and Döll [44]. Recently, Rossmanith [76] indicated that increasing crack tip bluntness is the contributing factor in enhancing the stress intensity factor which leads to branching. Dally et al. [8,32,56], showed the existence of a Γ-shaped plateau, which was considered a necessary condition for branching in the $C - K_{ID}$ relation, where K_{ID} is the dynamic fracture toughness. The experimental studies of dynamic crack propagation by

Ravi-Chandar and Knauss [77,78], indeed showed that a unique $C - K_{ID}$ relation did not exist, and that K_{ID} varied even though the crack velocity remained constant. Relations between crack velocity C and K_{ID} for different fracture test specimens of Fig. 2 show the "plateau", as well as the differences in plateau values which varied with specimen and loading conditions.

The stress wave hypothesis [48,79,80] requires strong interactions between the propagating crack tip and stress waves of large amplitudes. Carlsson [48] hypothesized that micro-cracks form when a tensile dilatational wave impacts the crack front and that the main crack could fork only in the presence of residual stresses. The stress wave hypothesis for crack branching is thus a plausible cause but is not a necessary condition for branching since available experimental results show crack branching without stress wave interaction [27,28,55].

2.2.3. The energy criterion

The energy rate criterion requires crack branching when the strain energy release rate exceeds the energy which is dissipated by a single propagating crack. Based on experimental studies, Johnson and Holloway [81,82] and Bansal [83] attributed branching to the excessive supply rate of the driving energy to the propagating crack tip. Recently, Rabinovitch [84] discussed the energy hypothesis of Johnson and Holloway [82] and of Bansal [83] and showed that their energy equations were not valid for a crack propagating at the limiting velocity. Eshelby's approach [85] to crack branching is also based on the energy balance at the onset of branching at a crack velocity larger than $0.3C_1$.

By examining the experimental results for different materials with identical specimen geometry, Rossmanith and Irwin [86] and Rossmanith [76] indicated that heat loss had to be accounted for in predicting crack branching. Fuller et al. [87] indeed observed the increase in temperature at the onset of crack branching.

2.3. Crack branching angle

Theories used to predict crack branching angles under static loading conditions are the maximum circumferential stress theory [88], the minimum strain energy density factor theory [89], and the maximum strain energy release rate theory [90–93]. Theoretically predicted branching angles based on static analyses are larger than the experimentally observed branching angles. Sih [94] predicted branching angle of 15–18 degrees under a pure mode I dynamic loading condition by using the minimum strain energy density criterion. Since this criterion is sensitive to variations in Poisson's ratios, it could be verified experimentally by examining crack branching data of different materials. By using the maximum stress criterion, Kalthoff [13] found that crack branches with a small branching angle tended to repel one another when $K_{II}/K_I > 0$. Also, branches with a large initial branching angle tended to attract each other when $K_{II}/K_I < 0$. Crack propagation along the original direction was possible when $K_{II} = 0$. The branching angles measured by Kalthoff agreed with his analytical prediction. Elastostatic solutions of Kitagawa et al. [95,96] and Vitek [97] arrived at a similar conclusion, where the crack branched with a branching angle of 18 degrees at zero K_{II} and agreed well with the analytical results of Lo [11].

The experimental results for the branching angle by Kalthoff [13] and those of A.S. Kobayashi [31] and Christie [98] indicate that the crack tip stress state governs the magnitude of the branching angle. Congleton [63] observed crack branching angles of about 40–80 degrees in a bursting steel pipe. Crack branching angles observed by Nakasa and Takei [99], Bullen et al. [100] and others in ceramics [101], all involve positive σ_{0x}, which resulted in larger crack branching angles in these experiments. Indeed, recent

experimental results on ceramics [74] showed that the remote tensile biaxiality yielded a larger crack branching angle.

3. Experimental evidences of advanced cracking

Fracture topography and high-speed photography show that fracture is a continuous process of crack initation and crack propagation [8,27,39,48,102–104]. Formation of secondary cracks, which grow with the advancing main crack tip, creates a region of energy dissipation and generates the roughness of the fracture surface. Figure 3 shows the dynamic photoelastic records of a fracturing Homalite-100 specimen just prior to, and at the moment of crack branching, as well as the evolution of multiple cracks which were subsequently generated under a higher crack tip stress field. Some secondary cracks do not link up with the main crack and stop growing after being passed over by the crack tip. Although all materials have an inherent array of microflaws, which grow and coalesce under load, the nucleation phase involving these secondary cracks prior to macro-crack growth is often neglected in the analysis.

The nature of the mirror, mist, and hackle regions on the fracture surface has been investigated as early as 1950 by Kies et al. [105,106] and in the late sixties by Johnson and Hollway [81]. The region of transition, mist, contained a number of geometries resembling parabolas or hyperbolas and semicircular "ribs" in the region of greatest roughness. Such geometries can be associated with an "advance" crack forming parallel to the main fracture plane and resulting in a rough fracture surface [107]. The generation of advance cracks ahead of the main crack was indeed observed by Ravi-Chandar and Knauss [39] in a high-speed photographic record of a fracturing Homalite-100 specimen. From this experimental observation, they concluded that the roughness of the fracture surface results from "independent" fracture origins, which generate the many parabolic and hyperbolic markings, at the front of the main crack. This experimental evidence of advance crack generation justify the use of advance cracks in modeling crack curving and branching mechanisms. Based on these experimental results, Ravi-Chandar and Knauss [39] proposed a mechanism for crack branching which, in essence, is similar to the authors' approach [30,108,109].

From the above brief review, the following salient observations are obtained:

1. No theoretical analysis on dynamic crack curving and branching is available.
2. The existence of the $C - K_{ID}$ plateau may be a necessary, but not a sufficient, condition for crack branching.

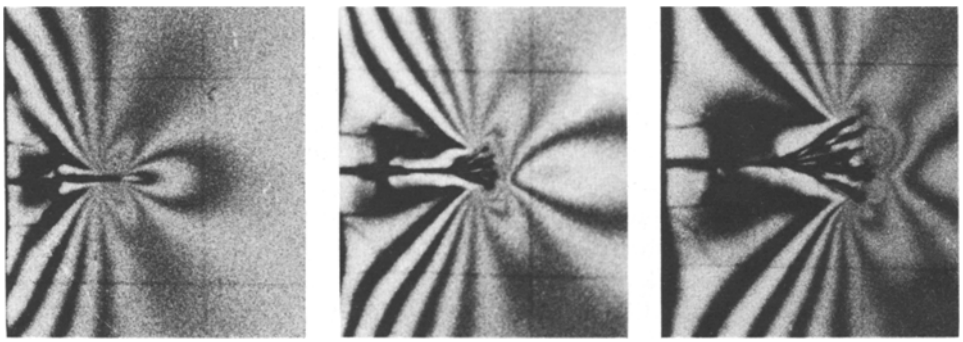

Figure 3. Incipient crack branching photoelastic record of Homalite-100 specimen.

Second frame, 37μ seconds Third frame, 71μ seconds Fourth frame, 103μ seconds

3. The branching stress intensity factor, K_{Ib}, could be a material property.
4. The crack branching angle, θ_c, could depend on the specimen geometry and loading.

4. Near field state of stresses of a rapidly running crack

The crack tip dynamic state of stress under mixed mode conditions was given by Freund and Clifton [110] and the general solution of a running crack was reported by Nishioka and Atluri [111] in terms of the local rectangular, (x, y), and polar coordinates (r, θ). Under pure mode I loading conditions (i.e., $K_{II} = 0$), the dynamic singular crack tip stress field for small θ values differs with the corresponding static stress field in that the largest (tensile) principal, singular stress component acts parallel to the x-axis not only in mode I loading but also in mixed mode loading for smaller values of K_{II}/K_I [30]. Furthermore, the biaxial stress ratio of σ_{xx}/σ_{yy} is roughly equal to unity for both static and dynamic loads up to $C/C_1 < 0.10$. The σ_{0x} term exists only in the σ_{xx} stress component of mode I loading, and is zero in all other components of mode I and mode II stress fields. Situations arise however, for which a single parameter, K_I, characterization of the crack tip stress field is not adequate due to the large spreading of the fracture process zone or the reduction in the size of the K-dominated singular zone [8]. Even in a brittle material, roughening of the fracture surface due to the spreading of the advance cracks and incipient branching can substantially enlarge the fracture process zone. In such cases, it is desirable to incorporate additional stress field parameters in order to characterize the stresses with those associated with a straight and sharp crack. This inevitable involvement of the higher order terms, forms the basis of the following crack curving and branching analyses of a moving crack.

The higher order terms in the crack-tip stress field not only initiate crack curving or branching but also influence their directions. The singular principal stress, σ_1, attains its maximum value at 60 degree with respect to the crack when the crack velocity $C/C_1 \to 0$, and shifts to 60-105 degrees with increasing crack velocity. The angular position of the maximum stress, unfortunately does not correlate with the experimentally observed crack curving or branching angles when additional higher order terms are introduced in computing the maximum stress. These poor correlations between the experimental and theoretical crack branching angles compel one to look at an alternative, the maximum circumferential stress, which is maximum at $\theta = 0$ and almost constant within $\theta = \pm 15$ degrees. This maximum circumferential stress will generate advance cracks when $C/C_1 < 0.32$ and will enhance openings of the off-axis micro-cracks which are located at a critical distance off the propagating crack tip.

5. Micro-mechanics of crack curving and crack branching

The hypothetical crack curving and crack branching mechanisms based on crack-tip micro-cracking is explained in the following [109]. First the micro-cracks nucleate from the inclusions and voids in the vicinity of the crack tip and grow as a result of the imposed crack-tip stress field. Continual crack growth results in coalescence of the micro-cracks in the crack-tip region and reduces the stress intensity factor by the increase in the compliance of the crack-tip core region. Simultaneously, the remote stress component, σ_{0x}, which acts parallel to the crack and which is the second order term in the crack-tip stress field, increases in magnitude [4,112]. The increased magnitude in the stress parallel to the crack in turn activates the microcracks away from the crack-tip plane. If the micro-cracks are sufficiently close to the main crack tip, they will tend to divert the crack away from its original plane [4,112–114]. A single crack-tip diversion results in crack curving and multiple crack-tip diversion results in crack branching. Also, with an increasing stress

intensity factor, the micro-cracks grow sufficiently large to engulf the main crack tip which now depicts a blunt crack. The larger energy release rate associated with the apparent blunt crack tip will in turn require the generation of branched cracks for larger energy dissipation. As a result, the main crack will extend through this damaged region and leave in its wake a series of distinct attempted branches [114]. At a sufficiently high applied stress intensity factor of K_I, the branched cracks will continue to propagate and thus complete successful crack branches [63]. In the foregoing cases, the necessary prerequisite for crack curving and branching is the growth of micro-cracks into macro-cracks with eventual hookup to the main crack. As shown in previous papers [19,30,108,109,115–117], the remote stress component, σ_{0x}, which is acting parallel to the direction of the crack propagation, controls the location and orientation of micro-cracking and hence governs the directional stability of an extending crack.

5.1. Dynamic crack curving

With the foregoing assumption that the advanced off-axis micro-cracks dictate the direction of crack propagation, either of the two dynamic crack curving criteria [30] by the authors, namely the maximum circumferential stress or the minimum strain energy density criterion, can be used to predict crack curving. Both criteria predict nearly identical crack curving angles in the experimentally observed crack velocity range and in the presence of "smaller" values of K_{II}. The angular position of the micro-cracks with respect to the crack tip, depends both on the micro-structure of the material and on the stresses at a characteristic distance, r_0, from the crack tip. These two parameters are linked together in a criterion involving the directional stability of an extending crack [30] and is a dynamic extension of Streit and Finnie's directional stability criterion [19] for quasi-statically extending crack.

The onset of crack curving of a rapidly propagating crack is governed by the stability of the propagating straight crack and is assumed to occur when $r_0 \leqslant r_c$. This r_c is a characteristic distance derived from the above-mentioned directional stability criterion which suddenly becomes unstable for $\sigma_{0x} > 0$ or in the presence of a smaller value of K_{II}. The corresponding angle, θ_c, for a maximum $\sigma_{\theta\theta}$, under a pure mode I dynamic crack extension can be determined through a transcendental relation involving the state of stress and r_c. The r_c associated with this directional stability model is assumed to be a critical material property and the crack will curve at the angle θ_c [30].

5.2. Dynamic crack branching criterion

The aforementioned micro-mechanics involved in crack curving and crack branching indicates that the crack branching criterion requires both a critical stress intensity factor that is accompanied by the characteristic distance $r_0 \leqslant r_c$. The crack branching criterion can thus be stated as:

$K_I \geqslant K_{Ib}$ Necessary condition

$r_0 \leqslant r_c$ Sufficient condition.

6. Recent experimental results

6.1. Dynamic crack curving in photoelastic specimens

The validity of the above crack curving criterion was verified by results involving photoelastic measurements on Homalite-100 specimens. Crack curving was consistently

observed in all of the above specimens when $r_0 \leqslant r_c$ and yielded an average value $r_c = 1.3$ mm at the onset of curving. A small K_{II} co-existed immediately after crack instability, possibly due to advance cracks, and changed the direction of crack propagation. Experimental details of this series of tests can be found in [14,16,20,30].

Further verification of this criterion was made by Sun et al. [115] with dynamic photoelastic experiments involving polycarbonate, double-edge crack tension specimens. Crack configurations involved were either offset parallel cracks, offset slanted cracks, and symmetrically located twin cracks which were used in this series of dynamic photoelastic study. The annealed thin polycarbonate specimens with blunt starter cracks exhibited brittle fracture with shear lips less than 10 percent of the thickness. At the onset of crack curving, the average r_c value was 0.5 mm which is consistent with the r_c estimated by Theocaris [118]. The theoretically predicted crack curving angles, either in pure mode I or modes I and II loading conditions, in the presence of σ_{0x}, were within one degree of the corresponding measured values.

6.2. Dynamic crack branching in photoelastic specimens

Crack branching criteria [108,109] require a critical stress intensity factor to trigger crack branching and a curving criterion to predict the crack branching angle. A review of all

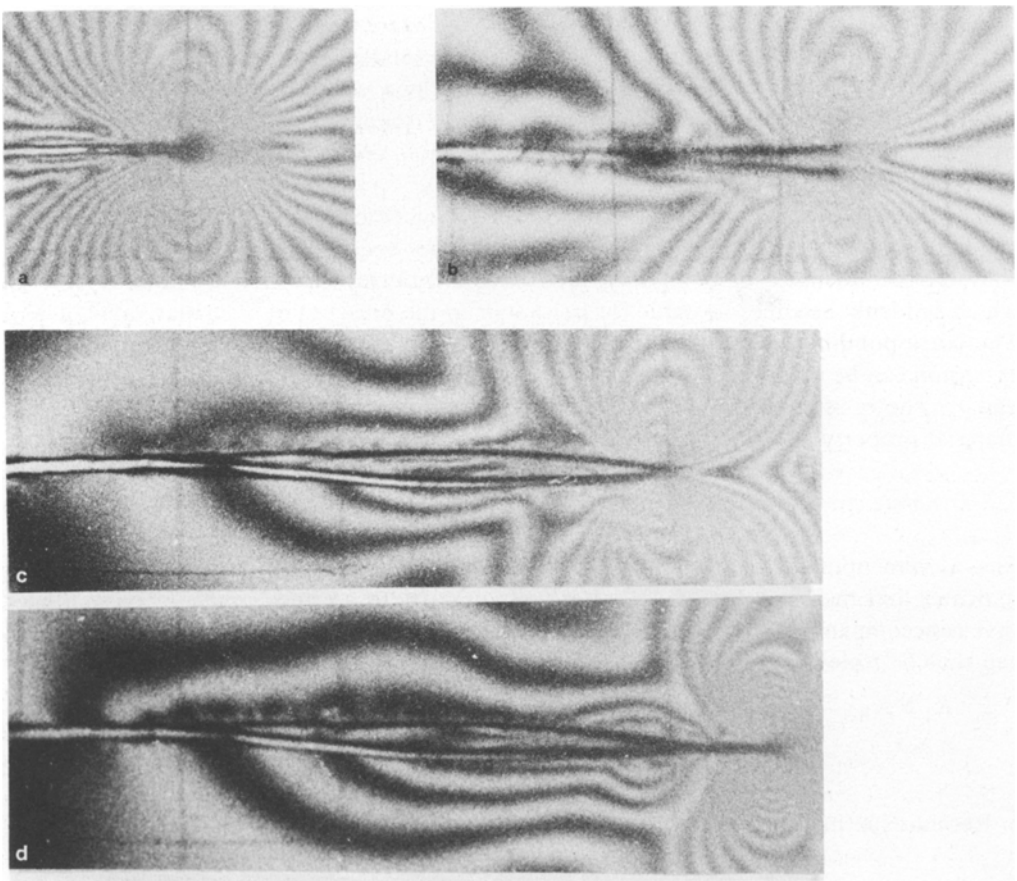

Figure 4. Typical dynamic-photoelastic record of crack branching in a polycarbonate single-edged-notch specimen. Specimen NO-RB-811003-01, (a) Eight frame, 83μ seconds. (b) Eleventh frame, 122 μ seconds. (c) Thirteenth frame, 151μ seconds. (d) Fourteenth frame, 174μ seconds.

past and recent crack branching data on Homalite-100 and polycarbonate photoelastic polymers involving SEN specimens showed that most cracks would bifurcate upon reaching a branching stress intensity factor.

The crack branching results of the Homalite-100 experiments [108] yielded an average r_c of 1.3 mm at branching and a $K_{Ib} = 2.04$ MPa$\sqrt{m}$. At the onset of crack branching, the crack velocities were found to be about 0.18 C_1. This K_{Ib}, which is approximately 4.9 times the fracture toughness of Homalite-100, is in agreement with the measured K_{Ib} of Dally [8].

Figure 4 shows five frames out of a 16-frame dynamic photoelastic record in a 3.2 mm thick, 127 × 127 mm polycarbonate SEN specimen with a blunt starter crack. No attempt was made to analyse these post-branched cracks, but at the onset of branching, $K_{Ib} = 3.2$ MPA$\sqrt{m}$ was obtained. It is interesting to observe in this experiment that the branching angle was 8 degrees and is less than the usually observed angles in the SEN specimens. After branching, post-branch cracks ran parallel and close to each other. These parallel cracks could have propagated together only if they were traveling at the same velocity. The slower of the two, however, arrested, as shown in [108]. The stress intensity factors of these two closely spaced cracks could not be determined since the interaction effects of the two cracks have not been incorporated into the data reduction process. The crack velocity at the onset of branching was found to be about 0.22 C_1 and is consistent with the other five crack branching experiments reported earlier [116].

In the SEN specimens, the energetic requirement of multiple cracking was satisfied but the crack curving criterion could not be satisfied since $\sigma_{0x} < 0$, $K_{II} = 0$. Under such a condition, $\sqrt{\xi}\,\sigma_{\theta\theta}/K_I$ is maximum at $\theta = 0$ for the crack velocity of $C/C_1 < 0.32$. However, the reduction in the angular stress distribution of $\sqrt{\xi}\,\sigma_{\theta\theta}/K_I$ at $\theta = \pm(10\text{-}14)$ degrees is a mere $1.7 - 3.5$ percent which allows the crack to bifurcate and double its energy release rate. Therefore, the predicted crack branching angle is at best an estimated angle [116].

The above-mentioned crack curving as well as the crack branching criteria were also verified in wedge loaded, rectangular double cantilever beam (WL-RDCB), Homalite-100, specimens [108,117], and in pressurized metal pipes of steel [119] and aluminum [120]. Predicted and measured branch angles in wedge loaded, rectangular double cantilever beam (WL-RDCB) specimens and bursting pipes were found to be in good agreement [108,109].

7. Discussions

High-speed photoelastic investigations [14,16] of crack curving reveal that this phenomenon is often associated with the backward tilt of the crack tip isochromatics. This tilt indicates positive values of remote stress, σ_{0x}, observed in dynamic tear test (DTT) specimens under impact loading and double cantilever beam (DCB) specimens under wedge loading. The proposed crack curving criterion predicts the curving angle well. Stress wave interaction and the resulting mixed mode effect also control the crack direction.

The direction of maximum $\sigma_{\theta\theta}$ at a critical radial distance is always at $\theta = 0$ for $\sigma_{0x} < 0$ and $C/C_1 < 0.32$. However, crack branching occurred at an average included crack branching angle of $2\theta_c = 28$ degrees when $C/C_1 < 0.32$ and when $\sigma_{0x} < 0$ in SEN specimens. The differences between the theoretical and experimental results can be explained by examining the instantaneous circumferential stress associated with the onset of crack branching at the critical radial distance. As discussed earlier, the reduction in circumferential stress at $\theta = \pm 14$ degrees is less than 3 percent for the observed crack velocity. Presumably, the propagating crack can extend in any direction within $\theta = \pm 14$ degrees in order to bifurcate and double its energy release rate. The averaged value of the

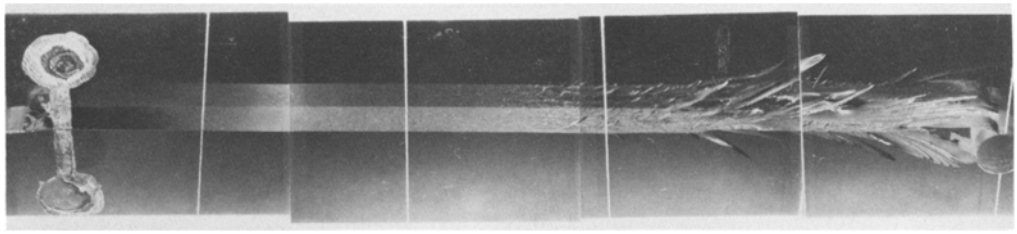

Figure 5. Typical fracture surface in Homalite-100 crack branching experiments.

estimated half-branching angle of 15.4 degrees in polycarbonate [116] and 14 degrees in Homalite-100 specimens is in good agreement with the measured half-branching angle. This agreement demonstrates that the crack branching criterion remains valid despite the predicted self-similar crack extension for $K_{ID} < K_{Ib}$. The calculated one-half branching angle with $\sigma_{0x} < 0$ is the best estimated angle under a pure mode I condition. The dynamic stress intensity factor at the onset of crack branching reached an average maximum value of 2.0 MPa$\sqrt{m}$ in Homalite-100, and 3.3 MPa$\sqrt{m}$ in polycarbonate fracture specimens. The branching stress intensity factors were found to be material-dependent.

The photoelastic patterns of running post-branched cracks in all of our experimental observations initially showed the effect of mixed mode and higher order terms. These results suggest that the crack will run parallel to the compressive stress direction and that the mixed mode isochromatics after branching appeared to be generated by the advance cracks. Therefore, postbranching crack propagation is dependent on the K_{II}/K_I ratio but also on σ_{0x} as well. The crack curving of Fig. 4 shows that the crack curving angle of both parallel running cracks gradually decreased so that the cracks curved toward each other and continued to propagate when the crack branching angle was 8 degrees. Although inconclusive, it appears from the available experimental results, that successful branching is possible only if $2\theta_c > 20$ degrees. For $2\theta_c < 20$ degrees, however, branched cracks merged with the main crack and propagated in accordance with Kalthoff's results [13].

Figure 5 shows the typical fracture surface in a 12-mm-thick Homalite-100 SEN specimen associated with crack branching with mirror, mist, and hackle regions. The mist, hackle, and crack branching show the nucleation of advance cracks which resulted in surface roughness [39]. Also, note that the microcracks do not span the entire plate thickness. Some exist on the two plate faces while others occur in the middle of the plate and are continuously curving prior to a successful crack branching. This fracture surface indicates that the σ_{0x} term is compressive and opens the micro-cracks in shear failure.

Work performed so far in dynamic crack curving and crack branching was primarily concerned with two-dimensional problems. In most engineering materials, crack growth, curving, and branching are locally three-dimensional problems associated with advance nucleations of micro-cracks. The high-speed photomicrographic experiments of Ravi-Chandar and Knauss [39,57], illustrate the three-dimensional effects in the nucleation of micro-cracks.

8. Conclusions

The review of the present and of the previous studies on crack curving and crack branching were presented. Criteria based on crack tip micro-mechanics proposed by the authors were used to predict the curving and branching in brittle materials.

Acknowledgement

The work reported here was obtained under ONR Contract NO-0014-76-C-000 NR-064-478. The authors wish to acknowledge the support and encouragement of Dr Y. Rajapakse, ONR, during the course of this investigation.

References

[1] J.D. Achenbach, in *Fracture Mechanics* XII SIAM-AMS Proceedings 12 (1979) 3–20.
[2] L.B. Freund, in *Mechanics of Fracture,* Edited by F. Erdogan, 19 ASME (1976) 105–134.
[3] F. Nilson, *SM Archives* 2 (1977) 205–261.
[4] L.R.F. Rose, *International Journal of Fracture* 12 (1976) 799–813.
[5] J.E. Field, *Contemporary Physics* 12 (1971) 1–31.
[6] M.F. Kanninen, in *Numerical Methods in Fracture Mechanics,* Edited by A.R. Luxmoore and D.R.J. Owen, University College of Swansea, UK (1978) 612–633.
[7] A.S. Kobayashi, in *Fracture Mechanics*, Edited by N. Perrone et al., University Press of Virginia (1978) 481–496.
[8] J.W. Dally, *Experimental Mechanics* 19 (1979) 349–367.
[9] B.L. Karihaloo, L.M. Keer and S. Nemat-Nasser, *Engineering Fracture Mechanics* 13 (1980) 879–888.
[10] B. Cotterell and J.R. Rice, *International Journal of Fracture* 11 (1981) 155–164.
[11] K.K. Lo, *Journal of Applied Mechanics* 45 (1978) 797–802.
[12] L.C. Pärletun, *Engineering Fracture Mechanics* 11 (1979) 343–358.
[13] J.F. Kalthoff, in *Dynamic Crack Propagation,* Edited by G.C. Sih, Noordhoff International Publishing (1973) 449–458.
[14] A.S. Kobayashi and C.F. Chan, *Experimental Mechanics* 16 (1976) 176–181.
[15] J.F. Kalthoff, in *Work Shop on Dynamic Fracture,* Edited by W.G. Knauss et. al., California Institute of Technology (1983) 11–35.
[16] A.S. Kobayashi, S. Mall and M. Lee, *ASTM STP 601* (1976) 274–290.
[17] J.J. Benbow and F.C. Roesler, *Proceedings of the Physics Society* London 70 B (1957) 201–211.
[18] B. Cotterell, *International Journal of Fracture Mechanics* 1 (1965) 96–103.
[19] R. Streit and I. Finnie, *Experimental Mechanics* 20 (1980) 17–23.
[20] W.B. Bradley, "A Photoelastic Investigation of Dynamic Brittle Fracture", Ph.D. thesis, University of Washington (1969).
[21] J.J. Kibler and R. Roberts, *Journal of Engineering for Industry* (1970) 727–734.
[22] J.C. Radon, P.S. Leevers and L.E. Culver, in *Fracture 1972,* 3, University of Waterloo Press (1977) 1113–1118.
[23] I. Finnie and A. Saith, *International Journal of Fracture* 9 (1973) RCR 484–486.
[24] B. Cotterell, *International Journal of Fracture Mechanics* 2 (1966) 526–533.
[25] B. Cotterell, *International Journal of Fracture Mechanics* 6 (1970) 189–192.
[26] M.L. Williams, *Journal of Applied Mechanics* 24 (1957) 109–114.
[27] K. Ravi-Chandar and W.G. Knauss, *International Journal of Fracture* 26 (1984) 141–154.
[28] K. Ravi-Chandar and W.G. Knauss, *International Journal of Fracture* 26 (1984) 189–200.
[29] B.L. Karihaloo, L.M. Keer, S. Nemat-Nasser and A. Oranatnachai, *Journal of Applied Mechanics* 48 (1981) 515–519.
[30] M. Ramulu and A.S. Kobayashi, *Experimental Mechanics* 23 (1983) 1–9.
[31] A.S. Kobayashi, B.G. Wade, W.B. Bradley and S.T. Chiu, *Engineering Fracture Mechanics* 5 (1974) 81–92.
[32] G.R. Irwin, J.W. Dally, T. Kobayashi, W.L. Fourney, M.J. Etheridge and H.P. Rossmanith, *Experimental Mechanics* 19 (1979) 121–128.
[33] J. Congleton and N.J. Petch, *Philosophical Magazine* 16 (1967) 749–760.
[34] S.R. Anthony and J. Congleton, *Metal Science* (1968) 158–160.
[35] S.R. Anthony, J.P. Chubb and J. Congleton, *Philosophical Magazine* 22 (1970) 1201–1216.
[36] F. Kerkhoff, in *Dynamic Crack Propagation,* Edited by G.C. Sih, Noordhoff International Publishing, Leyden (1973) 3–35.
[37] P.S. Theocaris, *Journal of the Mechanics and Physics of Solids* 20 (1972) 265–279.
[38] A. Shukla and S. Anand, "Crack Propagation and Branching Under Biaxial Loading," presented at 17th National Symposium on Fracture Mechanics, Albany, New York (August 1984).
[39] K. Ravi-Chandar and W.G. Knauss, *International Journal of Fracture* 26 (1984) 65–80.
[40] E.H. Yoffe, *Philosophical Magazine* 42 (1951) 739–750.
[41] J.W. Craggs, *Journal of the Mechanics and Physics of Solids* 8 (1960) 66–75.
[42] B.R. Baker, *Journal of Applied Mechanics* 29 (1962) 449–458.
[43] F.P. Bowden, J.H. Brunton, J.E. Field and A.D. Heyes, *Nature* 216 (1967) 38–42.
[44] W. Döll, *International Journal of Fracture* 11 (1975) RCR 184–186.
[45] H. Schardin, in *Fracture*, Edited by B.L. Averbach et al., John Wiley (1959) 297–330.
[46] P. Acloque, *Silicate Industrials* 28 (1963) 323–331.
[47] J. Carlsson, *Transactions of the Royal Institute of Technology, Stockholm* 189 (1962) 2–55.
[48] J. Carlsson, *Transactions of the Royal Institute of Technology, Stockholm* 205 (1963) 3–38.

[49] J. Carlsson, *Transactions of the Royal Institute of Technology, Stockholm* 207 (1963) 3–26.
[50] G.R. Irwin, *ASTM STP 627* (1977) 7–18.
[51] G.T. Hahn, R.G. Hogland and A.R. Rosenfield, in *Fracture 1977*, 2, University of Waterloo Press (1977) 1333–1338.
[52] R.J. Weimer and H.C. Rogers, in *Proceedings of the Second International Conference on Mechanical Behavior of Materials,* Boston (1976) 1473–1477.
[53] R.J. Weimer and H.C. Rogers, *Journal of Applied Physics* 50 (1979) 8025–8030.
[54] A.S. Kobayashi, in *Progress in Experimental Mechanics*, Edited by V.J. Parks (1975) 83–97.
[55] A.S. Kobayashi and M. Ramulu, *Experimental Mechanics* 21 (1981) 41–48.
[56] T. Kobayashi and J.W. Dally, *ASTM STP 627* (1977) 257–273.
[57] K. Ravi-Chandar and W.G. Knauss, in *Workshop on Dynamic Fracture*, California Institute of Technology (February 17-18 1983) 119–128.
[58] T.L. Paxson and R.A. Lukas, in *Dynamic Crack Propagation,* Edited by G.C. Sih, Noordhoff International Publishing, Leyden (1973) 415–426.
[59] M.S. Doyle, *Journal of Material Science* 18 (1983) 687–702.
[60] J.D. Achenbach, in *Prospects of Fracture Mechanics,* Edited by G.C. Sih et al., Noordhoff International Publishing (1974) 319–336.
[61] J.D. Achenbach, *Journal of Elasticity* 9 (1979) 113–129.
[62] A.B.J. Clark and G.R. Irwin, *Experimental Mechanics* 6 (1966) 321–330.
[63] J. Congleton, in *Dynamic Crack Propagation,* Edited by G.C. Sih, Noordhoff Publishing (1973) 427–483.
[64] R.A. Sack, *Proceedings Physics Society* London 58 (1946) 729–736.
[65] J.J. Mecholsky, R.W. Rice and S.W. Freiman, *Journal of American Ceramic Society* 57 (1974) 440–443.
[66] J.J. Mecholsky, S.W. Freiman and R.W. Rice, *ASTM STP* 645 (1978) 363–379.
[67] H.P. Kirchner and R.M. Gruver, *Philosophical Magazine* 27 (1973) 1433–1446.
[68] H. Kirchner and W.J. Kirchner, *Journal of American Ceramic Society* 62 (1979) 198–202.
[69] H.P. Kirchner, R.M. Gruver and R.E. Walker, *Journal of American Ceramic Society* 56 (1973) 17–21.
[70] J.J. Mecholsky, S.W. Freiman and R.W. Rice, *Journal of Material Science* 11 (1976) 1310–1319.
[71] H.P. Kirchner, R.M. Gruver, M.V. Swain and R.C. Garvie, *Journal of American Ceramic Society* 64 (1981) 529–533.
[72] A.I.A. Abdel-Latif, R.C. Bradt and R.E. Tressler, *International Journal of Fracture* 13 (1977) 349–359.
[73] K. Kishimoto, S. Aoki and M. Sakata, *Archives Mechanics* 33 (1981) 947–956.
[74] R.W. Rice, *ASTM STP 827* (1984) 5–103.
[75] A.S. Kobayashi and S. Mall, *Experimental Mechanics* 18 (1978) 11–18.
[76] H.P. Rossmanith, "Crack Branching in Brittle Materials Part I", University of Maryland Photomechanics Laboratory Report (1977–1980).
[77] K. Ravi-Chandar and W.G. Knauss, *International Journal of Fracture* 20 (1982) 209–222.
[78] K. Ravi-Chandar and W.G. Knauss, *International Journal of Fracture* 25 (1984) 247–262.
[79] B.R. Lawn and T.R. Wilshaw, *Fracture in Brittle Solids,* Cambridge University Press (1975) 100–104.
[80] H.P. Rossmanith and A. Shukla, *Experimental Mechanics* 21 (1981) 415–422.
[81] J.W. Johnson and G.W. Holloway, *Philosophical Magazine* 17 (1967) 899–901.
[82] J.W. Johnson and G.W. Holloway, *Philosophical Magazine* 19 (1966) 731–743.
[83] G.K. Bansal, *Philosophical Magazine* 35 (1977) 935–944.
[84] A. Rabinovitch, *Philosophical Magazine* 40 (1979) 873–874.
[85] J.D. Eshelby, in *Inelastic Behavior of Solids*, Edited by Kanninen et al., McGraw-Hill New York (1970) 77–115.
[86] H.P. Rossmanith and G.R. Irwin, "The Analysis of Dynamic Isochromatic Crack Tip Stress Patterns", University of Maryland Report (1979).
[87] K.N.G. Fuller, P.G. Fox, and J.E. Field, *Proceedings of the Royal Society* (London) A-341 (1975) 537–557.
[88] F. Erdogan and G.C. Sih, *Journal of Basic Engineering* 85(D) (1963) 519–527.
[89] G.C. Sih, in *Methods of Analysis and Solutions of Crack Problems* 1, Edited by G.C. Sih, Noordhoff International Publishing, Lyden (1973) 21–45.
[90] K. Palaniswamy and W.G. Knauss, in *Mechanics Today*, 4, Edited by S. Nemat-Nasser, Pergammon Press (1978) 87–148.
[91] M.A. Hussain, S.L. Pu, and J. Underwood, *ASTM STP 560* (1974) 2–28.
[92] C.H. Wu, *Journal of Applied Mechanics* 45 (1978) 553–558.
[93] H. Anderson, *Journal of the Mechanics and Physics of Solids* 17 (1969) 405–417.
[94] G.C. Sih, in *Elastodynamic Crack Problems,* 4, Noordhoff International Publishing, Leyden (1977) XVII-XLVII.
[95] H. Kitagawa, R. Yuuki and T. Ohira, *Engineering Fracture Mechanics* 7 (1975) 515–529.
[96] H. Kitagawa and R. Yuuki, in *Fracture 1977*, Edited by D.M.R. Taplin, 3, University of Waterloo Press (1977) 201–211.

[97] V. Vitek, *International Journal of Fracture Mechanics* 13 (1977) 481–501.
[98] D.G. Christie, *Transactions of the Institute of Glass Technology* 36 (1952) 74–89.
[99] K. Nakasa and H. Takei, *Engineering Fracture Mechanics* 11 (1979) 739–751.
[100] E.P. Bullen, F. Henderson and H. Wain, *Philosophical Magazine* 21 (1970) 689.
[101] R.E. Bullock and J.L. Kaae, *Journal of Material Science* 14 (1979) 920–930.
[102] W.B. Bradley and A.S. Kobayashi, *Experimental Mechanics* 10 (1970) 106–113.
[103] A.S. Kobayashi, S. Mall and W.B. Bradley, *Proceedings of the Twelfth Society of Engineering Science,* University of Texas at Austin (October 1975).
[104] A.S. Kobayashi and M. Ramulu, in *Mixed Mode Crack Propagation,* Edited by G.C. Sih and P.S. Theocaris, Sijthoff & Noordhoff (1981) 163–172.
[105] J.A. Kies, A.M. Sullivan and G.R. Irwin, *Journal of Applied Physics* 21 (1950) 716–720.
[106] I. Wolock, J.A. Kies and S.B. Newman, in *Fracture,* Edited by B.L. Averbach et al., Technology Press and Wiley (1959) 250–264.
[107] G.R. Irwin, in *Handbuch Der Physik* VI, Edited by S. Flugge, Springer-Verlag (1958) 551–590.
[108] M. Ramulu, A.S. Kobayashi and B.S.-J. Kang, *Fracture Mechanics* (15th), ASTM STP 833 (1984) 130–142.
[109] M. Ramulu, A.S. Kobayashi and B.S.-J. Kang, *Journal of Pressure Vessel Technology* 104 (1983) 317–322.
[110] L.B. Freund and R.J. Clifton, *Journal of Elasticity* 4 (1974) 293–299.
[111] T. Nishioka and S.N. Atluri, *Engineering Fracture Mechanics* 17 (1983) 1–22.
[112] J.R. Rice, *Journal of the Mechanics and Physics of Solids* 22 (1974) 17–26.
[113] J.R. Rice and M.A. Johnson, in *Inelastic Behavior of Solids,* McGraw Hill (1970) 641–672.
[114] R.O. Richi, J.F. Knott and J.R. Rice, *Journal of the Mechanics and Physics of Solids* 21 (1973) 395–410.
[115] Y.-J. Sun, M. Ramulu, A.S. Kobayashi and B.S.-J. Kang, in *Developments in Theoretical and Applied Mechanics,* Edited by T.J. Chung and G.R. Karr, The University of Alabama Huntsville (1982) 203–218.
[116] M. Ramulu, A.S. Kobayashi, B.S.-J. Kang, and D.B. Barker, *Experimental Mechanics* 23 (1984) 431–437.
[117] M. Ramulu and A.S. Kobayashi, *Engineering Fracture Mechanics* 18 (1983) 1087–1098.
[118] P.S. Theocaris and G. Papadopoulos, *Journal of Applied Mechanics* 49 (1982) 81–86.
[119] E.A. Almond, N.J. Petch, A.E. Wraith and E.S. Wright, *Journal of Iron and Steel Institute* 207 (1969) 1319–1323.
[120] R.W.E. Shannon and A.A. Wells, in *Proceedings of International Symposium on Pipeline,* Paper No. 17, Newcastle upon Tyne (1974).

Résumé

Une étude comparative sur les critères d'incurvation et d'arborescence d'une fissure en mécanique de rupture dynamique montre qu'un critère basé sur le concept de "fissuration avancée" présente la meilleure corrélation avec les données expérimentales disponibles. Le critère d'arborescence d'une fissure requiert comme condition nécessaire un facteur d'intensité de contrainte dynamique critique, K_{Ib}, et comme condition suffisante un critère tenant compte de l'incurvation de la fissure. Les critères sont utilisés pour prédire l'incurvation et l'arborescence d'une fissure au cours d'expériences photo-élastiques en condition dynamique mettant en oeuvre de l'Homalite 100 et du polycarbonate ainsi que des tubes d'acier et d'aluminium en cours d'explosion.